PAPER • **OPEN ACCESS**

Latent tracks of swift Bi ions in Si_3N_4

To cite this article: A Janse van Vuuren *et al* 2020 *Mater. Res. Express* **7** 025512

Materials Research Express

PAPER

Latent tracks of swift Bi ions in Si_3N_4

A Janse van Vuuren[1,13], A Ibrayeva[2,3], R A Rymzhanov[3,4], A Zhalmagambetova[4], J H O'Connell[1], V A Skuratov[4,5,6], V V Uglov[7,8], S V Zlotski[7], A E Volkov[4,9,10,11] and M Zdorovets[3,12]

[1] CHRTEM, NMU, University Way, Summerstrand, Port Elizabeth, South Africa
[2] L N Gumilyov Eurasian National University, Nur-Sultan, Kazakhstan
[3] Institute of Nuclear Physics, Almaty, Kazakhstan
[4] FLNR, JINR, Joliot-Curie 6, 141980 Dubna, Russia
[5] National Research Nuclear University MEPhI, Moscow, Russia
[6] Dubna State University, Dubna, Russia
[7] Belarusian State University, Minsk, Belarus
[8] South Ural State University, Chelyabinsk, Russia
[9] National Research Center 'Kurchatov Institute, Moscow, Russia
[10] Lebedev Physical Institute of the Russian Academy of Sciences, Moscow, Russia
[11] National University of Science and Technology MISiS, Russia
[12] Ural Federal University, Yekaterinburg, Russia
[13] Author to whom any correspondence should be addressed.

E-mail: arnojvv@gmail.com

Keywords: swift heavy ions, latent tracks, electron microscopy, x-ray diffraction, molecular dynamics simulation

OPEN ACCESS

RECEIVED
30 October 2019

REVISED
31 January 2020

ACCEPTED FOR PUBLICATION
4 February 2020

PUBLISHED
17 February 2020

Abstract

Parameters such as track diameter and microstruture of latent tracks in polycrystalline Si_3N_4 induced by 710 MeV Bi ions were studied using TEM and XRD techniques, and MD simulation. Experimental results are considered in terms of the framework of a 'core–shell' inelastic thermal spike (i-TS) model. The average track radius determined by means of electron microscopy coincides with that deduced from computer modelling and is similar to the track core size predicted by the i-TS model using a boiling criterion. Indirect (XRD) techniques give a larger average latent track radius which is consistent with the integral nature of the signal collected from the probed volume of irradiated material.

1. Introduction

The stability of solids against swift heavy ion irradiation (SHI) is usually related to the ability of projectiles to form latent tracks—highly disordered regions surrounding the ion trajectory. The experimental study of track-associated radiation damage has shown that the most important parameters are the electronic energy loss threshold above which the corresponding structural changes are revealed, and the track size. These two parameters are the only input data used for the verification of theoretical models of latent track formation. The threshold energy loss, S_{et}, and track radius, R_{tr}, may be determined by a variety of experimental techniques such as RBS/C, scanning force microscopy (SFM), profilometry, XRD, SAXS, Mössbauer spectroscopy and TEM. Recent analysis of data extracted from SHI irradiated YIG crystals using several techniques has revealed some discrepancy in the measured track radii depending on the characterization technique, whilst overall agreement for the electronic energy loss threshold was observed [1]. This emphasizes the importance of direct TEM observations for the determination of latent track parameters. Amongst materials with a definite lack of information about latent tracks from both direct and indirect techniques is polycrystalline silicon nitride. To date only a small amount of data on ion track associated radiation damage in this material is available [2–4].

Silicon nitride shows promise for nuclear applications such as inert matrix fuel host for the transmutation of long-lived radionuclides [5]. Materials with these applications must survive energy deposition due to neutron exposure, gamma and beta radiation, self-irradiation from alpha decay, and fission fragment damage. Fission fragment damage build-up and its consequences for material property changes remains poorly understood because it cannot be investigated using classical low-energy implanters. Bombardment with swift heavy ions

offers a unique opportunity to simulate fission fragment-induced damage. In this investigation swift Bi ion induced latent track size in Si_3N_4 measured by means of high-resolution STEM, XRD, molecular dynamic simulations and calculations within the framework of inelastic thermal spike model are compared.

2. Experimental

Commercially available polycrystalline β-Si_3N_4 obtained from MTI Corporation was used in this investigation. The specimens were irradiated with 710 MeV Bi ions (stopping power ≈36 keV nm^{-1}) to a fluence of 5×10^{11} cm^{-2} using the facility at the U-400 FLNR JINR cyclotron with an average ion flux 3×10^{8} cm^{-2} s^{-1}. Ion beam homogeneity over the irradiated specimen surface was controlled using beam scanning in the horizontal and vertical directions and was better than 10%. TEM lamellas oriented parallel to the implanted surface were prepared by means of an FEI Helios Nanolab 650. The lamellas were extracted from an area within the first 1 μm of the sample where the stopping power is highest and nearly uniform. To minimise ion beam induced damage the samples were prepared with ion energies down to 500 V. Structural analysis was done with a C_s corrected JEOL ARM200F transmission electron microscope operated at 200 kV.

X-ray diffraction analysis was carried out using Ultima IV diffractometer (Rigaku, Japan) in parallel beam geometry with CuKα radiation ($\lambda = 0.154179$ nm). X-ray patterns were recorded in a standard (θ–2θ) geometry from 10° to 80° with a step of 0.05° (2θ). The samples used in XRD studies were irradiated with fluences ranging from 5×10^{11} cm^{-2} to 1.23×10^{13} cm^{-2}.

3. Results and discussion

3.1. TEM examination

Determination of the size of Bi ion tracks by means of TEM is done from HAADF STEM images. This type of image is well suited for track measurement since contrast is related mostly to the projected average atomic number. Combined with the assumption of uniform specimen thickness (valid for the small area within the field of view) as well as uniform chemical composition (no compositional changes over the field of view), one may use the HAADF signal intensity as a measure of local material density. Since ion tracks are, in general, regions of lower density they will be visible as darker regions within the image. Images that contain several tracks (also dependent on the fluence) are collected and by analyzing the intensity profile the track diameter is measured. The diameter is taken as the FWHM of the area of lower intensity (density). The measurement process is illustrated in figure 1. Ideal images for such measurement are recorded at sampling intervals that do not produce sharp atomic column contrast in order to minimize high frequency intensity oscillation in the image. It should be noted that care is taken to account for tracks that are not in a perfectly planar orientation. In the case where tracks are at a slight angle the diameter is only measured perpendicular to the slant-direction. Several tracks are measured in this way and the average track diameter is then determined from these results.

In figure 2 a single ion track induced by the passage of 710 MeV Bi is shown in both annular bright field (ABF) and high angle annular dark field (HAADF) imaging modes in a crystal which is oriented in the [001] direction. The ABF image contains a larger contribution of diffraction related contrast whereas contrast in the HAADF image is related to average atomic number along the projected column. The darker areas in the ABF image are therefore most likely related to strain within the crystal, induced by irradiation. A region of slightly darker contrast can be seen to the top left of the amorphous track core, in the HAADF image, which is as a result of a slight angling of the track away from the imaging direction i.e. a part of the track lying within the lamella is also seen. The amorphous nature of the track core can clearly be seen in both images at the position of intersection of the track with the top surface of the lamella. Since STEM imaging is mostly sensitive to the top surface of the specimen, the crystalline lamella surface is superimposed on the track contrast in the region where the track is below the surface. The average track diameter for 710 MeV Bi ions in polycrystalline Si_3N_4 is 3.3 ± 0.3 nm.

3.2. XRD evaluation of latent track size

Figure 3 shows the XRD spectra of pristine and 710 MeV Bi ion irradiated specimens at increasing fluences. The spectrum obtained from the unirradiated material is composed of peaks related to the β-Si_3N_4 phase (P63).

The spectra in figure 3 indicate that structural changes in Si_3N_4 induced Bi ions only have an observable effect at fluences greater than 1×10^{12} cm^{-2}, whereas a further increase in fluence leads to the appearance of a wide halo corresponding to disordered silicon nitride. Accumulation of amorphous latent tracks and radiation damages also results in a shift of diffraction peaks toward smaller angles and in an increase in the width of diffraction peaks due to the growth of macro- and micro-stresses.

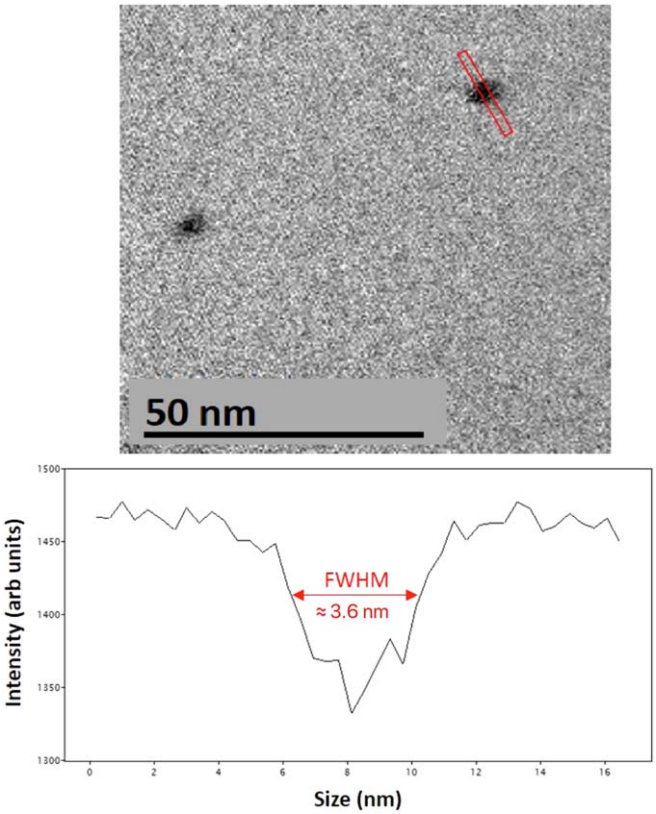

Figure 1. Illustration of how latent ion tracks are measured. The image on the upper is a HAADF STEM image with two tracks with an intensity profile from the track as indicated by the red rectangle. The profile itself is the bottom image.

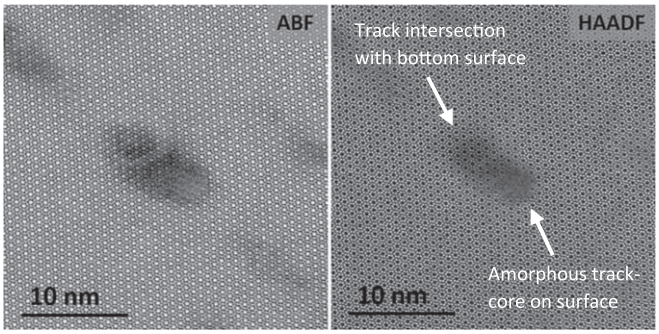

Figure 2. Complimentary ABF- and HAADF-STEM micrographs of a track which is in a slightly slanted orientation in Si_3N_4 irradiated with 710 MeV Bi to a fluence of 5×10^{11} cm^{-2}.

The damaged fraction, F_D, of SHI irradiated materials can be determined from the XRD patterns using the following equation [6]:

$$F_D = 1 - \frac{\sum_{i=1}^{n} \frac{A_i^{irradiated}}{A_i^{unirradiated}}}{n}$$

where $A^{irradiated}$ and $A^{unirradiated}$ are the net area of ith XRD line in the pattern obtained from irradiated and unirradiated samples, respectively, and n is the number of lines considered. Variation of $F_D$with the ion fluence can be found using the single impact model (Poison's relationship). The main idea of this approach is that every incident swift heavy ion creates an individual track and the overall damage observed at high fluences results from the overlapping of ion tracks [6]:

$$F_D = F_{max}(1 - e^{-S\Phi})$$

where F_{max} is a saturation level, S is an area with radius R_{track} surrounding the ion trajectory. The data calculated from the (200) XRD line and corresponding fitting line are shown in figure 4.. The effective X-ray penetration

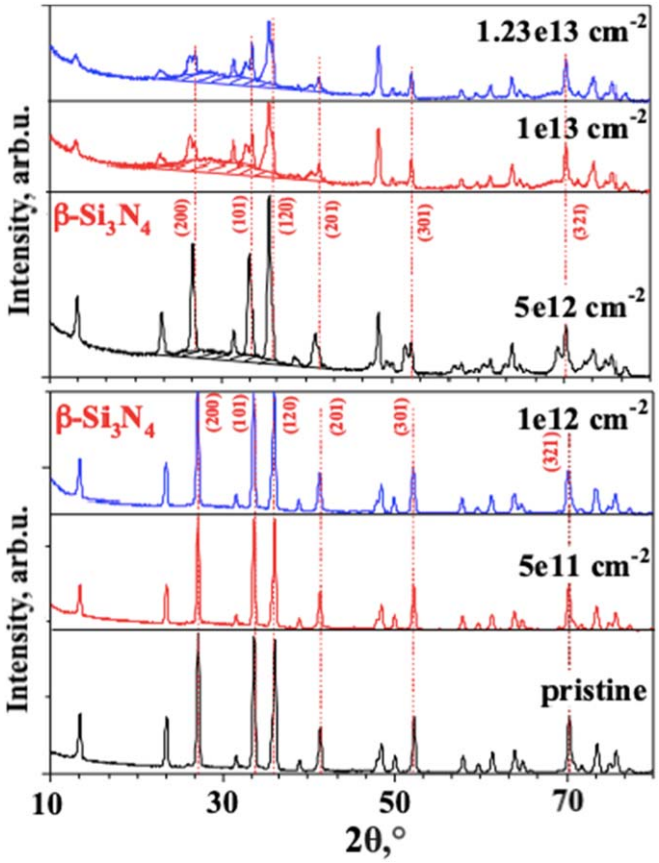

Figure 3. X-ray diffraction patterns of Si_3N_4 irradiated with 710 MeV Bi ions.

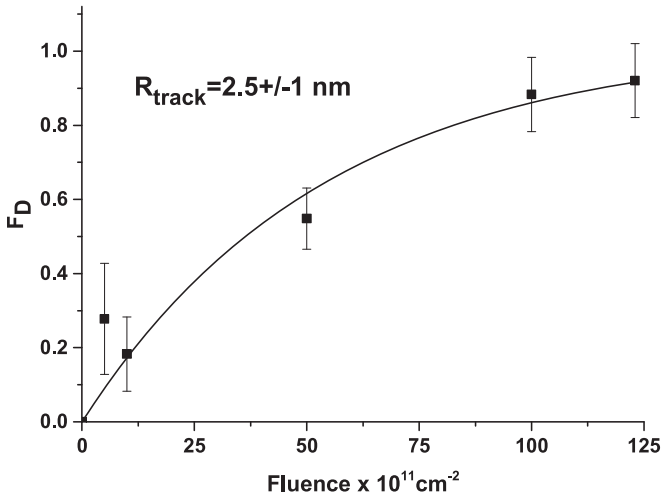

Figure 4. Damaged fraction versus 710 MeV Bi ion fluence.

depth of 27 μm is less than projected range for 710 MeV Bi ions which is 29.7 μm. From the parameters of the fitted-line function, the latent track radius is calculated to be $R_{\text{track}} = 2.5 \pm 1.0$ nm

3.3. MD simulation

To simulate the formation of Bi ion latent tracks a hybrid scheme was applied [7, 8] for the coupled kinetics of the excitation and relaxation of the electronic and the atomic sub-systems of a material irradiated with high-energy heavy ions. First, the asymptotic trajectory Monte Carlo code TREKIS [9, 10] is used to determine the initial parameters which are characteristic of an excited state of the ensemble of electrons as well as energy transferred to lattice atoms via electron-lattice coupling in an ion track. The calculated radial distribution of the

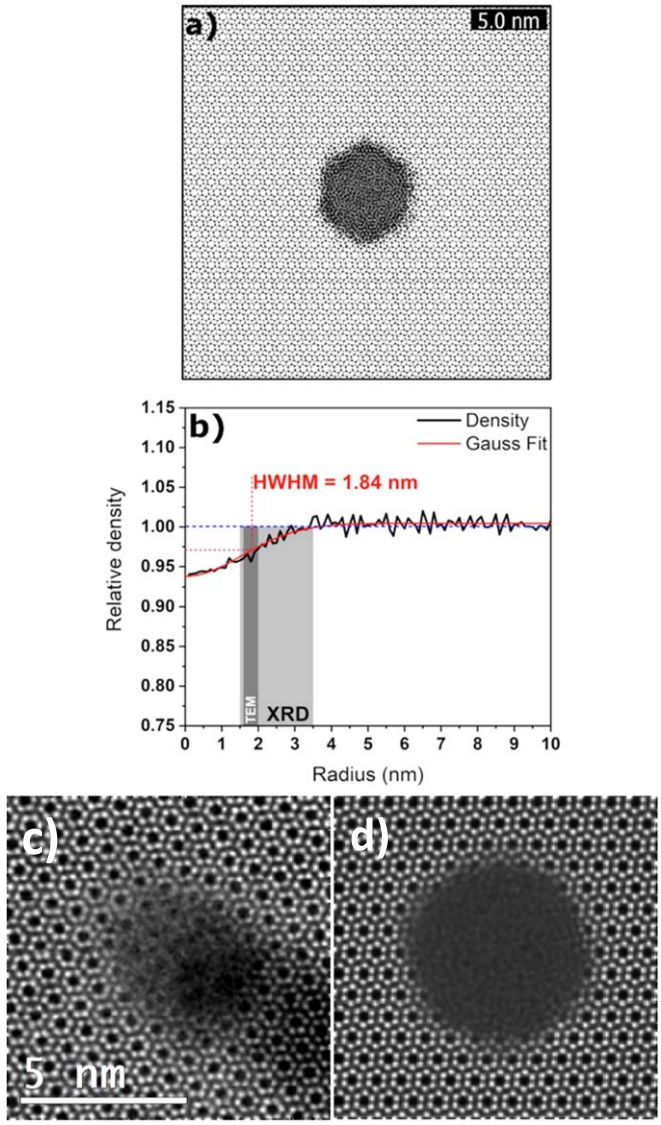

Figure 5. (a) Simulated ion track in silicon nitride at 150 ps after a passage of a Bi ion (710 MeV); (b) Normalized density variation as a function of radial distance from the track center as calculated from MD simulation. Grey rectangles show TEM and XRD track radius with errors. (c) Experimental HAADF image of slightly inclined track compared to (d) a simulated HAADF image from the MD simulation box.

energy transferred into the lattice is then used as input data for classical molecular dynamics code LAMMPS [11] used to simulate subsequent lattice relaxation and structure transformations appearing near the ion trajectory.

In MD simulations, the β-phase structure of Si_3N_4 is used. Interactions between atoms in Si_3N_4 are calculated using a Vashishta type potential with parametrization taken from [12]. All trajectories of projectiles were parallel to Z axis of the cell ([001] direction of Si_3N_4 lattice). The supercell sizes used in the MD simulations were $24.2 \times 23.5 \times 19.9\ nm^3$ (1096000 atoms) with the periodic boundary conditions in all directions. All details of the applied methods can be found in [7, 13]. Track evolution is traced up to 150 ps, after which the cell temperature dropped below 350 K, so no structural changes are expected after this time.

Figure 5(a) shows the simulated atomic snapshot of Si_3N_4 lattice in the nanometric vicinity of the trajectory of 710 MeV Bi ion at 150 ps after the SHI passage. The radial density profile calculated from MD results is shown in figure 5(b). The change of density can be observed within a radius of ~2.8 nm from the centre of the ion trajectory. The maximum decrease in the density is ~6% in the centre of the track. Fitting the radial density profile with a Gaussian function gives a FWHM of 3.68 ± 0.1 nm which may be taken as the track diameter. This yields a radius of 1.84 nm which is similar to the experimental value of 1.8 ± 0.2 nm obtained from TEM analysis. Figure 5(c) shows an experimental HAADF STEM micrograph of a slightly inclined track at the same scale as a simulated HAADF STEM micrograph (d) from the MD simulation cell in (a). Simulation was performed using MuSTEM software [14] with observation parameters similar to those during experimental observation. Probe convergence was 21 mrad with a detector collection angle of 54–85 mrad. C_s was set to 4 μm

and 0 μm defocus. No other aberration coefficients were set. The image is in reasonable agreement with HRSTEM micrographs. The simulated track shows slightly sharper boundaries and a slightly larger diameter, however, experimentally observed tracks had a diameter spread of almost 1 nm and the inclination results in a softer boundary as would be the case for perfect track alignment with observation direction. It should also be noted that the simulation cell thickness was around half the thickness of the observed specimen.

Despite the larger average track radius deduced from XRD analyis, it is possible that the data overlaps due the large scatter in data found from MD and TEM.

3.4. i-TS analysis

The inelastic thermal spike model has successfully been used to explain the effects of dense ionization in many dielectrics irradiated with swift heavy ions [15, 16]. The conventional i-TS model is known as an approach for explaining latent track formation as a result of quenching of molten matter resulting from extremely large amounts of energy deposited via electronic excitations in the region surrounding ion trajectory. This model is presented using two coupled differential equations [15]:

$$C_e(T_e)\frac{\partial T_e}{\partial t} = \frac{1}{r}\frac{\partial}{\partial r}\left(rK_e(T_e)\frac{\partial T_e}{\partial r}\right) - g(T_e - T_i) + A(r, t)$$

$$C_a(T_a)\frac{\partial T_a}{\partial t} = \frac{1}{r}\frac{\partial}{\partial r}\left(rK_a(T_a)\frac{\partial T_a}{\partial r}\right) + g(T_e - T_a)$$

There C_e, C_a are specific heat capacities, T_e, T_a are temperatures, K_e, K_a are specific thermal conductivities (the indices *i* and *e* refer to the atomic (lattice) and electronic subsystems of the material, respectively), *A (r,t)* is the space-time source, describing the heating of the electronic subsystem of material by an incident ion.

Relatively good agreement between the predictions of the i-TS model and experimentally determined track radii is observed in many materials, especially in those where a crystalline-to-amorphous phase transition is observed i.e. so called amorphizable materials [16]. Since ion tracks, in Si_3N_4, induced by Bi ions show amorphous features, the first approach is to consider the 'melting' criterion, which assumes that a latent track will form in a volume where the lattice temperature is higher than the melting temperature [16]. The calculations performed with the only free parameter; the electron-phonon interaction mean free path $\lambda = 4.3$ nm, as is recommended for amorphizable inorganic insulators [16], yields a track radius of approximately 5 nm. This value is much larger than that obtained from TEM and MD analysis, irrespective of the approach of track size determination. One of possible reasons for this divergence may be the partial recrystallization of the distorted/disordered lattice, however some investigations have shown that recrystallization does not play significant role in track formation processes in amorphizable materials [8].

MD simulations show evidence of a slight shrinkage (recrystallisation) of track radius from 3.6 nm after 1 ps to 2.8 nm after 150 ps, but even this 'initial' radius is still significantly less than the i-TS prediction. Although TEM results suggest that Si_3N_4 is an amorphizable material the i-TS model based on the 'melting' criterion is unable to predict a value for track radius which matches experimental and MD results within an acceptable margin.

Kitayama et al [17] suggested that the evaluation of track sizes in silicon nitride may be achieved within the framework of a two-threshold i-TS model using two free parameters: electron-phonon interaction mean free path λ and boiling energy E_b. In this model the boiling phase energy is the threshold for core formation and the melting phase energy for shell formation.

Unfortunately, to our knowledge, no information regarding the evaporation/boiling temperature and the latent heat of fusion is available for silicon nitride. The boiling energy E_b is therefore set equal to 1.6 eV nm^{-1} after fitting of the track radius versus the electronic stopping power as determined from TEM analysis [4, 18, 19]. The calculation of the time evolution of the lattice temperature in silicon nitride in a radial distribution from the Bi ion path (figure 6) demonstrates that the size of region where the boiling temperature is reached, i.e. the track core radius, is equal to 2 nm. The existence of a shell around the track core in crystalline Si_3N_4 has not been definitively proven, however some suggestion of the presence thereof has been observed during STEM analysis but is not yet conclusive and warrants further future investigation. This suggests that latent track core radii in polycrystalline Si_3N_4 irradiated with high energy heavy ions can be predicted by the i-TS model using the threshold energy $E_b = 1.6$ eV/atom.

The improved fit of the results when assuming a two-threshold i-TS with a 'boiling' criterion suggests that either this is in fact the mechanism which facilitates track formation in Si_3N_4, or it is possibly not a truly amorphizable material. Since the vaporisation temperature is unknown it is possible that the assumptions regarding what constitutes the boiling energy is inaccurate.

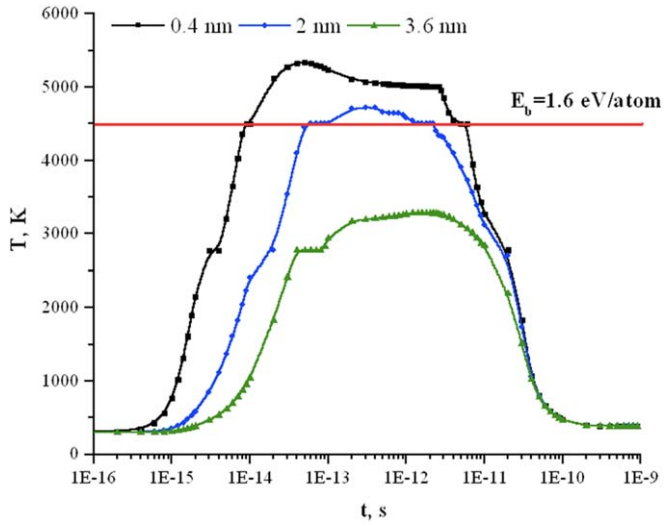

Figure 6. Temperature evolution at different radial distances from the Bi ion axis in Si_3N_4.

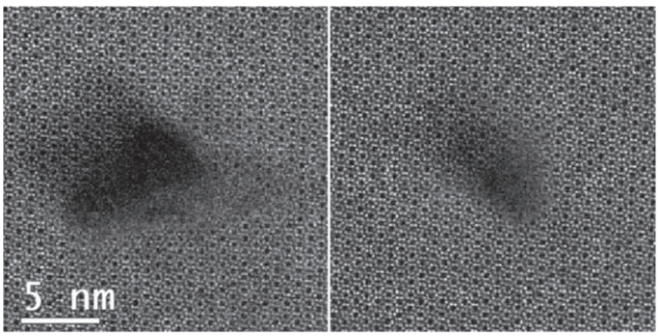

Figure 7. Individual track sizes appear larger in regions of semi-overlap (left) than for isolated tracks (right).

4. Conclusions

In this investigation the effective track diameters due to 710 MeV Bi ions in Si_3N_4 were measured using direct imaging by TEM, indirect inference through XRD as well as numerically via MD. The measurement technique, as explained, for HAADF STEM images was employed as an easily repeatable standard that can be used to compare results of different experiments in a reproducible manner. The technique also lends itself to easy automation to further improve the repeatability and avoids the issue of a gradual transition from amorphous phase to pristine crystal complicating defining the edge of the track. In fact, HAADF contrast is proportional to Z^n where $1.6 < n < 1.9$. This is close enough to 2 so that we can approximate the local density of a uniformly thick and constant composition lamella as proportional to the square root of HAADF intensity. In practice, the FWHM of a low density zone produced by a SHI is similar when measured on the raw image and the square root of the image and since the value of half maximum was chosen arbitrarily, we use the raw image for simplicity. Since TEM allows direct visualization of the ion track, this measurement serves as our benchmark to compare to other results while keeping in mind that different techniques are sensitive to different levels of 'distortion' of the pristine lattice. For the XRD measurements, it is clear that the total amorphous fraction generated by fluences up to 10^{12} cm^{-2} is too low to detect using our setup. At 5×10^{12} cm^{-2}, appreciable track overlap is already present due to the random positioning of ion impacts. Semi-overlapping impacts lead to damage multiplication as shown in figure 7.

Regions of closely spaced semi-overlapping tracks show significantly more damage (larger amorphous volumes) than the sum of two well separated tracks. This observation is consistent with current models on track formation in that regions of pre-existing damage should have lower thermal conductivity and higher electron-phonon coupling leading to higher temperature spikes during impact. For this reason, one may assume that on average, track diameter slightly increases with pre-existing damage levels. Equivalently, average track diameter should increase slightly with fluence, especially for materials that show a degree of recrystallization after initial

excitation. This suggests that a pure poisson fit to the amorphous fraction versus fluence plot is probably not perfectly accurate since the S is actually a function of Φ, i.e. $S = S(\Phi)$. Also, since XRD is sensitive to slight lattice parameter shifts, it probably 'sees' larger track radii due to lattice strain around the underdense core. Even so, our measurements show that the inferred track size from XRD overlap with that from TEM within experimental uncertainty. Very good agreement was found between MD simulated track sizes and those from TEM when the FWHM of the density profile was considered as a size indicator. This suggests that the employed potential and initial energy deposition can reasonably approximate the excitation and relaxation process in Si_3N_4. Assuming a two-threshold (liquid-vapour) i-TS model, it is possible to predict a track core radius consistent with experiment and MD simulation with the assumption that 'boiling' leads to amorphous track formation. There is however a certain amount of uncertainty regarding these assumptions since the exact evaporation/boiling temperature of Si_3N_4 is unknown. It appears as if a better fit is obtained if a two threshold i-TS and a 'boiling-phase' criterion is assumed. However, additional analysis including a better understanding of the physical properties of Si_3N_4 may be required.

ORCID iDs

A Janse van Vuuren https://orcid.org/0000-0002-5372-1149
R A Rymzhanov https://orcid.org/0000-0002-7404-9769
J H O'Connell https://orcid.org/0000-0002-3758-3997
V A Skuratov https://orcid.org/0000-0002-9016-8370

References

[1] Meftah A, Benhacine H, Benyagoub A, Grob J, Izerrouken M, Kadid S, Khalfaoui N, Stoquert J, Toulemonde M and Trautmann C 2016 *Nuclear Instruments and Methods in Physics Research section B: Beam Interactions with Materials and Atoms* **366** 155
[2] Zinkle S, Skuratov V and Hoelzer D 2002 *Nuclear Instruments and Methods in Physics Research section B: Beam Interactions with Materials and Atoms* **191** 758
[3] Janse van Vuuren A, Skuratov V, Ibraeva A and Zdorovets M 2017 *Proc. of the 12-th Int. Conf. of Interaction of radiation with solids IRS-2017* p 114
[4] Janse van Vuuren A, Skuratov V, Ibrayeva A and Zdorovets M 2019 *Acta Physica Polonica A* **136** 241
[5] Kleykamp H 1999 Selection of materials as diluents for burning of Plutonium fuels in nuclear reactors *Journal of Nuclear Materials* **275** 1
[6] Moll S, Sattonnay G, Thome L, Jagielski J, Legros C and Monnet I 2010 *Nuclear Instruments and Methods in Physics Research section B: Beam Interactions with Materials and Atoms* **268** 2933
[7] Rymzhanov R, Medvedev N and Volkov A 2017 *Journal of Physics D: Applied Physics* **50** 475301
[8] Rymzhanov R, Medvedev N, O'Connell J, Janse van Vuuren A, Skuratov V and Volkov A 2019 *Scientific Reports* **9** 3837
[9] Medvedev N, Rymzhanov R and Volkov A 2015 *Journal of Physics D: Applied Physics* **48** 355303
[10] Medvedev N, Rymzhanov R and Volkov A 2016 *Nuclear Instruments and Methods in Physics Research section B: Beam Interactions with Materials and Atoms* **388** 41
[11] Plimpton S 1995 *Journal of computational physics* **117** 1
[12] Walsh P, Omeltchenko A, Kalia R, Nakano A, Vashishta P and Saini S 2003 *Applied Physics Letters* **82** 118
[13] Rymzhanov R, Gorbunov S, Medvedev N and Volkov A 2019 *Nuclear Instruments and Methods in Physics Research section B: Beam Interactions with Materials and Atoms* **440** 25
[14] Allen L, D'Alfonso A and Findlay S 2015 *Ultramicroscopy* **151** 11
[15] Toulemonde M, Paumier E and Dufour C 1993 *Radiation Effects and Defects in Solids* **126** 201
[16] Toulemonde M, Dufour C, Meftah A and Paumier E 2000 *Nuclear Instruments and Methods in Physics Research section B: Beam Interactions with Materials and Atoms* **166** 903
[17] Kitayama T *et al* 2015 *Nuclear Instruments and Methods in Physics Research section B: Beam Interactions with Materials and Atoms* **356** 22
[18] Ibrayeva A, Janse van Vuuren A, O'Connell J, Skuratov V and Zdorovets M 2019 *20th Int. Conf. of Radiation Effects in Insulators* p 157
[19] Ibrayeva A, Janse van Vuuren A, O'Connell J, Skuratov V and Mutali A 2019 *Proc. of the 13-th Int. Conf. of Interaction of radiation with solids IRS-2019* p 97